Materials Chemistry and Physics 185 (2017) 129–136

Contents lists available at ScienceDirect

Materials Chemistry and Physics

journal homepage: www.elsevier.com/locate/matchemphys

Evaluation of process influences on surface chemistry of epoxy acrylate based solder mask via XPS, ToF-SIMS and contact angle measurement

Caroline Hofmeister [a, b, *], Sebastian Maaß [a], Thorsten Fladung [b], Bernd Mayer [b]

[a] Robert Bosch GmbH, Postfach 30 02 40, 70442 Stuttgart, Germany
[b] Fraunhofer Institute for Manufacturing Technology and Advanced Materials IFAM, Wiener Str. 12, 28359 Bremen, Germany

HIGHLIGHTS

- A surface model describing the process influences is proposed.
- Detailed siloxane reaction analysis was possible with ToF-SIMS.
- Photo-chemical, chemical and thermal surface modification occur during PCB manufacturing.

ARTICLE INFO

Article history:
Received 30 October 2015
Received in revised form
10 October 2016
Accepted 13 October 2016
Available online 14 October 2016

Keywords:
Surface properties
Ageing
Polymers
XPS
Heat treatment

ABSTRACT

Epoxy acrylate based solder mask formulations were conditioned by different printed circuit board (PCB) manufacturing and PCB assembly process stages. Depending on these different influences the chemistry of the solder mask surface was investigated regarding adhesion to possible adhesion partners. The combination of X-ray photoelectron spectrometry (XPS), time-of-flight secondary ion mass spectrometry (ToF-SIMS) and the contact angle method, for surface energy determination, provided a detailed understanding of the surface near region up to the topmost monolayer, which forms the contact zone in which adhesion takes place. The combination of ToF-SIMS and XPS provided molecular information of surface components comprising quantitative information. The influences of all process steps, like UV, chemical and thermal treatment, on the chemical surface composition and appearance were identified. Based on the results a chemical surface model could be created regarding the different adhesion mechanisms. It has been shown that an enrichment of siloxanes at the surface is generated by different mechanisms that were distinguished based on ToF-SIMS. Even though an oxidation process in the surface near region (10 nm) was indicated by XPS, no increase of the surface polar groups and thus no polarity increase could be observed within the first monolayer. A surface model derived from the analysis results shows generation and occupation of free sites at the surface through all stages of the process. An occupation of free sites by siloxanes from additives in the solder mask formulation results in a siloxane dominated topmost monolayer.

1. Introduction

Solder masks are used in printed circuit board (PCB) technology to provide defined soldering geometries and protect circuitry mechanically. The PCB is exposed to many influences within the PCB manufacturing and PCB assembly process. Among PCB assembly and production of the electronic device, adhesive bonding of different adhesion partners, as e.g. thermal conductive and sealing adhesives or encapsulations, to the solder mask surface takes place. For this purpose, the solder mask provides the surface at which adhesion is supposed to occur. After the solder application, different process stages within the PCB manufacturing and assembly are passed. These process influences are acting at the solder mask surface and a modification of the solder mask surface chemistry might occur. Regarding the adhesion function, the interaction between the solder mask surface and the chemical and thermal influences of different process steps must be understood,

* Corresponding author. Robert Bosch GmbH, Postfach 30 02 40, 70442 Stuttgart, Germany.
E-mail address: caroline.hofmeister@de.bosch.com (C. Hofmeister).

http://dx.doi.org/10.1016/j.matchemphys.2016.10.015
0254-0584/

since adhesion is dominated by just a nano scaled contact zone which in turn is highly influenced by manufacturing conditions. A reliability issue for electronic devices is generated, if a loss of adhesion results in delamination between the PCB and the adhesive.

The IPC-HDBK-840 (Institute for Interconnecting and Packaging Electronic Circuits-Solder Mask Handbook) describes photoimageable solder mask as epoxy acrylate resin mixtures. They are used to create a structured solder mask film at the PCB. Due to the different curing mechanisms of epoxies and acrylates, two different network structures result, which are statistically mixed [1]. But IPC-HDBK-840 also describes sophisticated solder mask systems, with tailored backbone molecules [1]. This was realized by the pre reaction to oligomers, like Park et al. described [2]. So fully, partially and non epoxidized acrylates result.

Fig. 1 summarizes the solder mask application, PCB manufacturing and assembly process steps. After application via spray or curtain coating of the epoxy acrylate mixture, radical polymerization of the acrylate compound is induced by UV radiation and generates a polymeric network on the exposed areas. At unexposed areas, via UV-absorbing photo mask, the radical polymerization is not induced and thus these regions can be resolved with a developing solution. Additional cross linking is achieved by latent curing agents during a subsequent thermal step. An additional UV treatment of the cured solder mask after thermal curing is applied for increased resistance of the surface. In literature the degradation of many polymeric systems due to an UV radiation is known, which can result in polymer chain breaking, photo-oxidative degradation, radical reactions, transformation reactions and reduction of molecular weight [3–7]. Depending on the wave length used during the UV radiation, homolytic cleavage of chemical bonds might occur. Selective bond breaking, rearrangements and bimolecular reactions are the consequences. The effect of a special kind of UV treatment must be evaluated for the UV treatment parameters and the treated polymeric system.

Within the PCB manufacturing, bare copper surfaces, at which the soldering process takes place, are passivated to avoid corrosion. The kind of passivation, also called final finish, could be of organic or inorganic nature. Typical final finishes are the metallic preservative immersion tin (iSn) [8] and the Organic Solderability Preservative (OSP) [9]. The coating process on copper surfaces occurs in wet bath chemistry under acid and basic conditions. During application of the final finish, the solder mask is also exposed to the specific wet bath chemistry. For this purpose, a possible modification of the solder mask surface due to residues must be taken into account.

During the electronic assembly the PCB undergoes a soldering process, at which temperature and process atmosphere (1000 ppm oxygen) act on the solder mask surface. Thermally induced degradation of polymeric systems is known in literature [10,11] and must be investigated for the solder mask system under soldering process conditions.

Within this study, the chemical surface appearance of solder mask material conditioned by different processes of the PCB manufacturing and the PCB assembly was investigated by combination of the surface sensitive techniques X-ray photoelectron spectrometry (XPS), time-of-flight secondary ion mass spectrometry (ToF-SIMS) and the contact angle measurement. With XPS quantitative information about the elemental composition of the first 10 nm of the surface can be obtained [12]. Since only binding states are detected with this method, ToF-SIMS is needed for characterization of the molecular structure [13,14]. Thus, the binding states of the XPS result can be correlated to specific components of the multi component solder mask system. The third method applied, contact angle measurement, allows determination of the surface energy and is highly sensitive to the first monolayer [15]. Combining these methods, a distinct characterization of the solder mask surface chemistry from the surface near region (10 nm) up to the topmost monolayers (1–3 nm) can be achieved. Regarding the various models of the adhesion theory known from literature [16–21], the method combination applied in this study derive the chemical and thermodynamic aspects [22]. Regarding the presence of siloxane based additives within the solder mask formulation, the segregation behavior at the surface depending on the processes carried out, must be understood, since additive segregation was stated by Hinder et al. [23]. Furthermore, siloxanes at surface can affect negatively the following adhesion to an adhesive, which is necessary in PCB processing [24].

2. Experimental

2.1. Materials

A commercially available, for automotive use typical solder mask system was utilized in this study. The basic chemistry of the solder mask was an epoxy acrylate dual cure system (bisphenol-A epoxy and methyl methacrylate) with a typical photoimageable solder mask formulation, including photoinitiators, thermal curing agents, silica-fillers, pigments and several organic solvents. Additionally, the solder mask formulation contained additives like PDMS (Poly(dimethyl)siloxane)-based anti-foaming and wetting agents. These are introduced to impact specific properties during

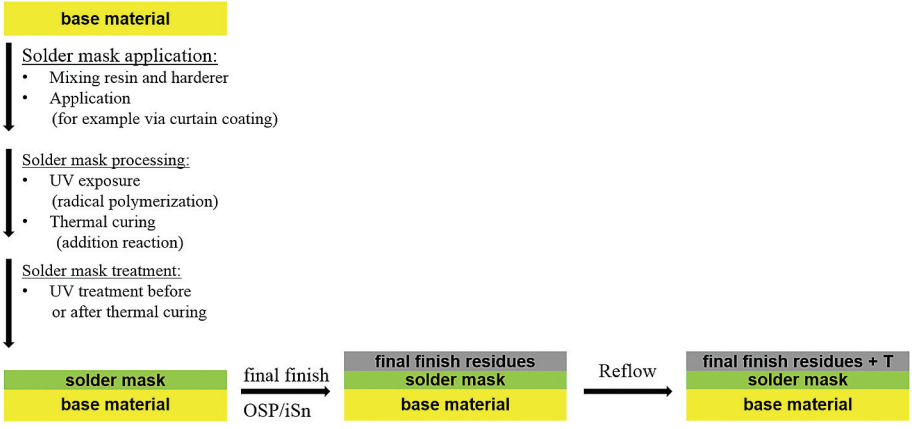

Fig. 1. Solder mask application, PCB manufacturing and assembly process steps.

the application e.g. in a curtain coating process [1]. Application on base material (consisting of glass fiber mats embedded with epoxy resin) was performed regarding manufacturer's recommendations, exhibiting process steps like UV-exposure, development and thermal curing as described by Park et al. [2].

2.2. UV treatment

UV treatment was performed with a medium pressure mercury lamp with a line spectrum in the range from 200 nm to 600 nm (energy peak at 365 nm and 254 nm) with an intensity of 200 mW/cm^2 under ambient conditions. Time was varied in order to receive different energy doses: 2000 mJ/cm^2 and 4000 mJ/cm^2. The UV treatment was carried out before and after the thermal curing of the solder mask at solder mask surface applied on base material and bare copper.

2.3. Chemical treatment

The solder mask surface was exposed to two different passivation (also called final finish) bath chemistries during the passivation of bare copper surfaces for corrosion inhibition. The commercially available Organic Solderability Preservative (OSP) based on benzimidazole chemistry [9,25] and the metallic equivalent immersion tin (iSn) [26] were used. Within both passivation steps, the copper surface was first cleaned by an acid cleaner and micro etched by a sulfuric acid solution. After the passivation stage the surface was rinsed with deionized water and dried. Additional rinsing steps between the micro cleaning, micro etching and passivation were carried out.

2.4. Thermal treatment

For PCB-conditioning the samples were exposed to a two stages thermal pretreatment. This simulates the thermal impact on the solder mask during the PCB assembly. The so called reflow-oven was a Hotflow 2/24 (ERSA GmbH, Germany). Two different temperature profiles were used, shown in Fig. 2, exhibiting maximum temperatures of 292 °C (245 °C solder mask surface temperature) and 310 °C (260 °C surface temperature) in the oven in a 1000 ppm oxygen atmosphere. Line speeds were 800 mm/min and 850 mm/min.

2.5. Characterization

2.5.1. X-ray photoelectron spectroscopy (XPS)

Quantitative information about the sample composition was gained from XPS measurements utilizing an Escalab 220i-XL-system (Thermo VG Scientific Ltd., UK) with a monochromatic X-ray source (Al-K_α). In the constant analyzer energy mode, 70 eV pass energy for survey spectra and 20 eV for high resolution line spectra (for example for C 1s and Si 2p region spectra), were used. C 1s and Si 2p peak-fitting were performed using synthetic Gaussian-Lorentzian components (70% and 30%) with a linear background subtraction. Analysis area has a diameter of approx. 0.65 mm. Information depth can be varied from 10 nm (perpendicular incidence) to 5 nm (angle of incidence 50°).

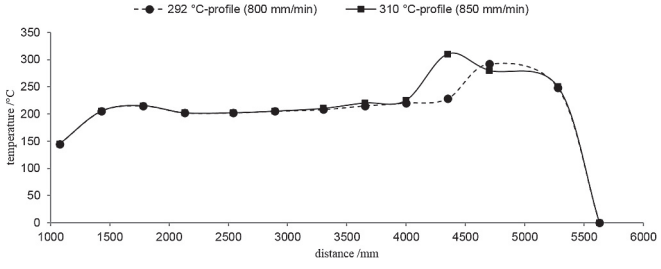

Fig. 2. Oven temperature profiles for PCB-conditioning.

2.5.2. Time of flight secondary ion mass spectroscopy (ToF-SIMS)

ToF-SIMS measurements were performed using a TOF-SIMS IV instrument (ION-TOF GmbH, Münster, Germany) in the static mode. Mass analysis provided by a time of flight mass analyzer, sputtering with a Bi_1^+ ion source (25 keV) and charge compensation by a pulsed electron flood gun. Positive and negative ion mass spectra in the mass range of 0–800 m/z were acquired from a measurement area of 500 μm × 500 μm. For data analysis the mass range of 0–400 m/z was used since the information content is pronounced in this mass range. The surface sensitivity of the ToF-SIMS method is about 1–3 monolayers. Depth profiling with TOF-SIMS was carried out with a separate sputter gun (Ar-cluster, 3 keV) in the interlaced mode. The spectra were recorded when the sputter gun is not operating.

To identify a species by TOF-SIMS, all physically feasible fragments of this specific component have to be characterized. Identification was accomplished by deducing potential fragments from the chemical formula and by library and a mass calculator of the Ionspec software. The normalized intensity derives semi-quantitative information about the occurring species and can be determined by the ratio to the total counting rate.

Due to the amount of fragments of one component, representative fragments were selected for the data interpretation, if all relevant fragments showed the same behavior.

Reproducibility of the solder mask surface was confirmed by distribution patterns (5 mm × 5 mm) with ToF-SIMS. For this purpose, three samples were measured two times and exhibited a homogeneous component distribution of the identified species in all cases. Due to the homogeneity of the sample surface and the quality of the peak fits, proven by standard deviation calculation of six different spectra, the number of ToF-SIMS measurements was limited to two repetitions, each with positive and negative polarization. Correlation of the ToF-SIMS measurements with the respective surface energy measurements, including standard deviations, and the XPS results confirmed that no deviations within one sample type occurred.

2.5.3. Surface energy analysis (sessile drop)

The surface energy analysis were performed by contact analysis [22] using an EasyDrop standard (Krüss GmbH, Hamburg, Germany) with Drop Shape Analysis DSA1 software equipment. Three fluids were used with the sessile drop method, water for HPLC from Sigma-Aldrich (CAS: 7732-18-5), diiodomethane with 99% purism from Sigma-Aldrich (CAS: 75-11-6) and ethylene glycol with p.a. > 99.5% (GC) from Fluka Analytics (CAS: 107-21-1). Utilizing the OWRK-method [27] the total polar and disperse parts of the surface energy were determined. For this purpose, nine single drops of each fluid were applied on the sample surface and the contact angle was measured. The surface sensitivity of sessile drop is one monolayer.

3. Results and discussion

3.1. Initial state

Performing XPS measurement of the initial state prior to any process influence except solder mask application, a surface composition of 42.7 at% carbon in aliphatic and aromatic compounds, 1.2 at% silicon in silica-filler (SiO_2), and 1.2 at% silicon in

PDMS (SiO) can be determined. Concerning polar components caused by the epoxy acrylate chemistry, 19.9 at% oxygen and 28.7 at % carbon are present in the solder mask surface near region. ToF-SIMS positive and negative spectra reveal a PDMS dominated surface. Fig. 3 illustrates a part of a representative positive spectrum of the coating surface, extracted from the chemical mapping.

All spectra are dominated by the PDMS-characteristic fragments listed in Table 2 for the positive polarization. In Fig. 4, the representative model of the chemical surface initial state (i.e. after solder mask application prior to further processing) is presented. In contact to air, a siloxane surface is covered by methyl groups and the polar oxygen is oriented into the bulk phase [28]. Additionally, polar fragments, which were deduced from base chemistry of the epoxy acrylate polymer, were identified (Table 1).

Depth profiling based on dynamic-SIMS (Ar^+ cluster, 3 kV, 70 nA) and angular resolved XPS, to reach 5 nm and 10 nm information depth, confirmed the assumption of an enrichment of PDMS in the surface near region. Furthermore, surface energy measurement showed a mainly non polar surface with low polar group content due to a high disperse part of the total surface energy of 40 mN/m and a low polar part of 1 mJ/m^2. Fig. 4 summarizes the XPS, ToF-SIMS and contact angle measurement results to a schematic surface model of the initial state of the epoxy acrylate system.

3.2. UV treatment

Regarding a photo degradation, the UV treatment of the above specified initial state was investigated. Generally, photo degradation may occur as e.g. photo oxidation, chain scission or crosslinking [3]. Thus, the photo oxidation generates a complex mixture of different products. Initially, free radicals are produced and lead to chain propagation (hydroperoxidation may occur), chain branching (chain scission may occur) and termination (crosslinking may occur). Dominating mechanisms are chain scission and crosslinking, but chain scission being predominant in the presence of oxygen [3]. Fig. 5 shows the XPS and contact angle results of the UV treated surface states: the PDMS content as contribution to the Si1s XPS peak (Fig. 5 (a)), the O/C ratio of polar surface groups (Fig. 5 (b)) and the surface energy (Fig. 5 (c)). Since UV sequence, weather it is performed before or after the thermal curing of the solder mask, has no influence on the surface chemistry, the mean values and the standard deviation includes both sequence types of UV treatment. Additionally, the mean values include measurements of solder mask applicated on base material and bare copper since it is known that a copper layer underneath affects not the surface chemistry of the solder mask (excepted the content of the copper itself) [30].

The O/C ratio represents polar and non-polar components of the solder mask. The maximum relative rise was about 12%. This rise is

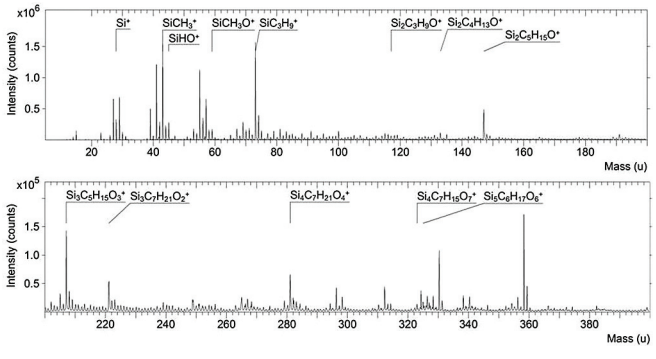

Fig. 3. ToF-SIMS positive spectrum of a representative sample. PDMS characteristic peaks are indicated.

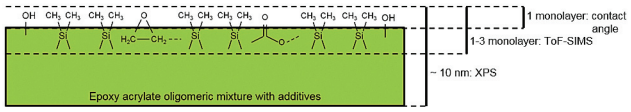

Fig. 4. Schematically description of the surface near region of the solder mask. The different information depth of the surface sensitive methods contact angle measurement, ToF-SIMS and XPS is displayed.

generated by UV intensity of 200 mW/cm^2 and an energy dose of 2 J/cm^2. Comparing the O/C change within the ranges 0–2 J/cm^2 and 2–4 J/cm^2 the ratio exhibited no prominent change by an energy dose of 4 J/cm^2. Israeli et al. [31,32] investigated the photo degradation of PDMS within a UV treatment with wavelengths $\lambda > 300$ nm. They described a hydroperoxidation of dimethylene groups and a photoscission of hydroperoxide groups into silanol groups. Also the transformation of SiH groups into silanol (SiOH) groups was observed. Based on ToF-SIMS analysis no transformation of siloxane ($SiO(CH)_x$) into silanol (SiOH) takes places. Additionally, XPS results exhibited constant SiO_2 amounts during the UV treatment originating from silica fillers. Based on this observations, the oxygen functionalities from PDMS (SiO) and fillers (SiO_2, $BaSO_4$) are not included within the O/C ratio, as this might falsify the degree of oxidation. This was carried out by discounting the O contributions from the mentioned components from the O1s XPS peak. Thus, an evaluation of the resin system without the contribution of PDMS based additives and fillers was possible.

Displayed in Fig. 5 (a), the siloxane amount increased with UV intensity of 200 mW/cm^2 and both energy doses (2 J/cm^2 and 4 J/cm^2). Corresponding to the siloxane increase the surface energy decreased (Fig. 5 (c)), while the surface topmost monolayers are PDMS dominated [33]. No increase of the surface energy polar part due to the oxidation observed with XPS was measured confirming a PDMS dominated surface layer of 1–3 nm.

ToF-SIMS should confirm the rise of PDMS and the change in polar surface functionalities in conformity with the XPS and surface energy results. Necessary requirement is an equal increase of fragments within one specie (for example all listed fragments of PDMS in Table 1 show an increase). But ToF-SIMS measurements showed that short PDMS fragments (mass 43–73 u; Table 1) exhibited an increase in the normalized intensity with UV energy dose of 2 J/cm^2, while long PDMS fragments (mass 117–325 u; Table 1) exhibited no change in the normalized intensity. With an energy dose of 4 J/cm^2, the short PDMS fragments exhibited no change and the long PDMS fragments showed an increase of the

Table 1
Secondary ion fragments of PDMS [29] on the left hand side and secondary ion fragments of polar components deduced from the base chemistry of epoxy acrylate on the right hand side.

Secondary ion fragment	Mass/(u)	Secondary ion fragment	Mass/(u)
Si^+	28	$C_2H_3O^+$	43
$SiCH_3^+$	43	$C_2H_5O^+$	45
$SiHO^+$	45	$C_3H_5O^+$	57
$SiCH_3O^+$	49	$C_4H_7O^+$	71
$SiC_3H_9^+$	73	$C_4H_7O_2^+$	87
$Si_2C_3H_9O^+$	117	$C_8H_8O^+$	120
$Si_2C_4H_{13}O^+$	133	$C_7H_{13}O_3^+$	145
$Si_2C_5H_{15}O^+$	147	$C_{16}H_{16}O^+$	224
$Si_3C_5H_{15}O_3^+$	207	$C_{16}H_{16}O_2^+$	240
$Si_3C_7H_{21}O_2^+$	221		
$Si_4C_7H_{21}O_4^+$	281		
$Si_4C_9H_{27}O_3^+$	295		
$Si_4C_7H_{15}O_7^+$	323		
$Si_5C_6H_{17}O_6^+$	325		

Table 2
Secondary ion fragments of the final finish residues, based on final finish chemistry [9].

Secondary ion fragments (OSP)	Mass/(u)	Secondary ion fragments (iSn)	Mass/(u)
Cu^+	63	$^{116}Sn^+$	116
$^{65}Cu^+$	65	$^{118}Sn^+$	118
$C_3H_4NS^+$	86	Sn^+	120
$C_3H_2Cu^+$	101	SnO^+	136
$C_7H_6N^+$	104	$SnOH^+$	137
$C_5H_5N_2S^+$	125		
$C_6H_5N_2Cu^+$	168		
$C_{10}H_7SN_3Cu^+$	264		

normalized intensity (see Fig. 6 (a) and (b)), but not significant in case of normalized intensities measured with ToF-SIMS. Summarizing, short and long PDMS fragments exhibited no change due to a rise in UV energy dose to 4 J/cm^2. Awaja et al. [34] described a chain scission mechanism of an epoxy resin due to UV treatment investigated with ToF-SIMS. Changes in the fragmentation pattern indicate a structural change. The deviation in the normalized intensities of short and long PDMS fragments corresponds to a chain scission. Relating the normalized intensities of short and long fragments for visualizing the chain scission mechanism, the reduction of long chains due to the increase of short chains can be described with the ratio of $Si_4C_9H_{27}O_3^+/SiC_3H_9^+$. Fig. 6 (c) shows, that the reduction takes place caused by an UV energy dose of 2 J/cm^2.

The polar fragments exhibited a decrease due to UV treatment (see Fig. 7 (a)), while the change in the normalized intensity of short polar fragments is greater than the change of long fragments. Fig. 7 (b) illustrates that the change of the $C_6H_9O^+/CH_3O^+$ ratio, representative for the ratio of all long to short fragments, is not based on a chain scission mechanism.

ToF-SIMS showed changes of the surface network structure by UV treatment of I = 200 mW/cm^2 and E = 2 J/cm^2. Due to an increase of the energy dose to E = 4 J/cm^2 no changes occurred, indicating that chain scission is dominated by the intensity influence. The disordered network structure allows the migration of the PDMS specie in the surface near region, increasing the SiO amount measured by XPS. As a result, the surface energy decreases since the surface energy of pure PDMS is in the range of 20 mN/m [33]. The energy for migration is contributed from the energy dose generating an increase of the sample surface temperature [3]. These observations are similar to the investigations of Truica-Marasescu et al. [35], which described a hydrophobic recovery via

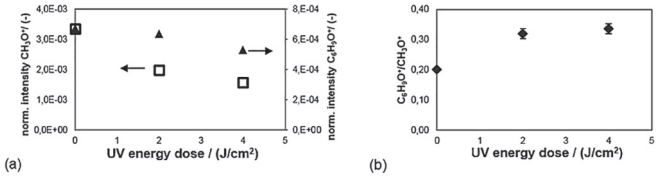

Fig. 7. ToF-SIMS: (a) Different normalized intensities of short (left hand side) and long (right hand side) polar groups (see Table 1). (b) A chain scission mechanism analogous to PDMS can be excluded.

restructuring of polyolefin surfaces within a VUV treatment. While XPS indicated an increase of bound oxygen, ToF-SIMS results showed a "loss" of functional groups and a surface energy decrease. In this context, an oxidation of the epoxy acrylate network takes place, but also the migration of the low molecular weight PDMS to the surface and the reorientation of polar groups into the bulk phase. Before the UV treatment takes place, so called initially PDMS is present at the sample surface, sourcing from PDMS based additives. Since this initially PDMS undergoes chain scission during the UV treatment, the disturbed network structure is more open for PDMS migration.

Summarizing the results of the UV treatment investigations, a photo-oxidation in the 10 nm surface region takes place, but is covered by PDMS within the top most monolayers, so the contact angle exhibited a surface energy decrease. Due to disordered network structure of PDMS monolayers and the thermal impact, both generated by UV treatment, the siloxanes migrate to the surface. The UV treatment generates photo-oxidation, chain scission and hydrophobic recovery in different depths of the surface region.

3.3. Chemical treatment

The influence of the final finish bath chemistry on the solder mask surface chemistry was investigated with XPS and ToF-SIMS. Following iSn application, a Sn content of <1 at% was detectable. For the OSP configuration the organic OSP residues could not be distinguished from the organic binding states of the numerous solder mask compounds by XPS due to the variety of components in the system. Nevertheless, utilizing ToF-SIMS it was possible to identify final finish residues on the sample surface by their characteristic fragments as displayed in Table 2. No quantitative assumptions may be based on XPS data, still, ToF-SIMS provides semi-quantitative information.

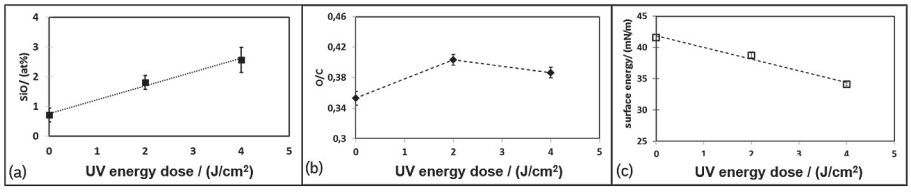

Fig. 5. XPS and surface energy of UV treatment with constant UV intensity (I = 200 mW/cm^2) and increasing UV energy dose: siloxane amount (a), O/C ratio (b) and surface energy (c). Dashed lines to guide the eyes.

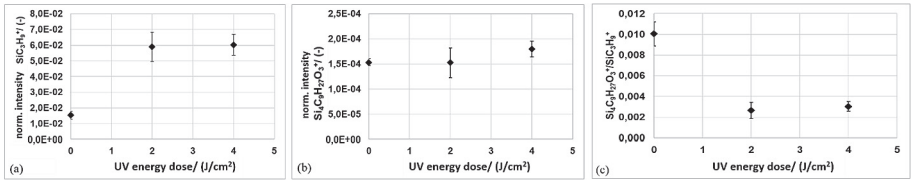

Fig. 6. ToF-SIMS: Different normalized intensities of short (a) and long (b) PDMS fragments (see Table 1). (c) Chain scission takes place with I = 200 mW/cm^2 and E = 2 J/cm^2.

OSP residues based on benzimidazole [9] and iSn residues were identified. Additionally, for OSP the corresponding copper-benzimidazole [36] complex was verified. Since the whole molecular structure of the benzimidazole $C_{10}H_7SN_3Cu^+$ was identified in the positive spectra, the OSP type with benzimidazole structure was verified. For iSn also tin isotopes were found. These results lead to the conclusion that the solder mask surface is contaminated by final finish residues after the final finish process, though thorough rinsing with distilled water is done after each process stage during PCB manufacturing. Additionally, changes in occupancy by PDMS and final finish residues were observed within the thermal treatment, which is discussed in the following section.

3.4. Thermal treatment

Comparing the solder mask surface chemistry in the initial state and processed with a final finish, changes in the siloxane amount were observed by XPS and ToF-SIMS. The normalized intensity of $SiC_3H_9^+$ (PDMS) depending on the various configurations is shown in Fig. 8. Without any processing (abbr.: no FF, no Reflow) the solder mask surface exhibited low normalized intensity of $SiC_3H_9^+$. Regarding this initial state, the OSP passivation generated no significant changes (abbr.: OSP, no Reflow), while the iSn passivation (abbr.: iSn, no Reflow) generates an increase of the $SiC_3H_9^+$ normalized intensity. During the thermal treatment with two different profiles (Reflow (292 °C) and Reflow (310 °C)) the $SiC_3H_9^+$ normalized intensities exhibited changes depending on the passivation type. The OSP processed surfaces exhibited significant increase, while iSn processed surfaces exhibited no significant change in the $SiC_3H_9^+$ normalized intensities. A one-way ANOVA (analysis of variance) with significance test (comparison of the mean values within the standard deviations for significant differences) and Tukey-Test (multiple comparison method with error level of 5%) was carried out for both, the characteristic final finish residue and the $SiC_3H_9^+$ normalized intensity, the latter representative for PDMS occupancy. The OSP residues and the resulting PDMS occupancy exhibited significant differences due to thermal treatment (Reflow), but no significant difference between the reflow treatments at 292 °C and 310 °C can be seen. In case of iSn residues, no significant differences due to the reflow treatment could be observed.

Regarding the changes of the identified OSP and iSn residues based on ToF-SIMS analysis (see Fig. 9), the normalized intensity of OSP residues decreased during thermal treatment (Fig. 9 (a)), while the normalized intensity of iSn residues exhibited no significant change (Fig. 9 (b)). The thermal stability of iSn residues and a thermal instability of OSP residues is obvious. Since an oxidation of iSn surfaces during the reflow thermal treatment is known [37], Tong et al. [9] stated a OSP layer decomposition temperature of 250°. Additionally, TGA and DSC measurements of pure benzimidazoles exhibited a melting temperature at 221 °C soon followed by commencing volatilization [38]. Based on these facts, it seems that the thermal instability of OSP residues results from evaporation of the benzimidazole, whereas iSn residues remain on the surface.

Taken the standard deviation into account the Si contribution to the siloxane content, measured with XPS, after thermal treatment was approx. 1 at% larger in the OSP configuration (3,2 at% Si) compared to the iSn configuration (2,1 at%), where no change in the siloxane content was observed. Hence, the siloxane content at the surface depends not only on the mobility of the siloxanes in the system, but also on available free sites at the surface, depending on the thermal stability of the characteristic final finish residue. Based on angle resolved XPS results, more siloxanes were pushed to the surface due to the thermal treatment and increased the siloxane content in the surface near region. Additionally, depth variation confirmed the enrichment of siloxanes in the surface near region, showing an increase of siloxane with decreasing information depth. Change in the siloxane content is approx. 1 at%.

Displayed in Fig. 10, comparing with the initial state, the surface energy of iSn and OSP processed surfaces decrease with increasing $SiC_3H_9^+$ normalized intensity. Data include configurations with and without thermal treatments. The increase in $SiC_3H_9^+$ normalized intensity is generated by thermal treatment, as also displayed in Fig. 8. OSP configurations exhibited a successive decrease in the surface energy, while iSn configurations showed a value leap from 37 mN/m to 30 mN/m due to thermal treatment with the reflow profile at 310 °C. In spite of the difference in Si contribution to siloxane content of at last 1 at% between the OSP and iSn configurations, the surface energies exhibited no significant difference.

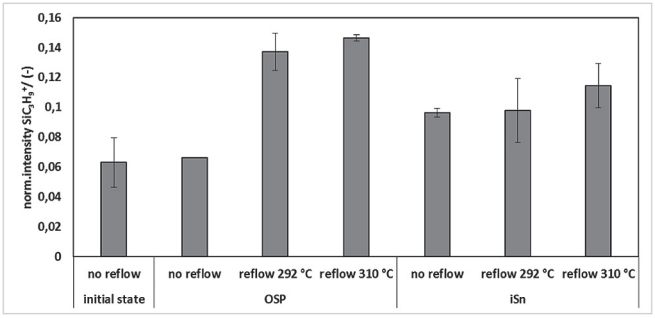

Fig. 8. ToF-SIMS: Changes in normalized intensity of $SiC_3H_9^+$ (PDMS) due to a processing of the solder mask surface with passivation (OSP and iSn) and thermal treatment (reflow).

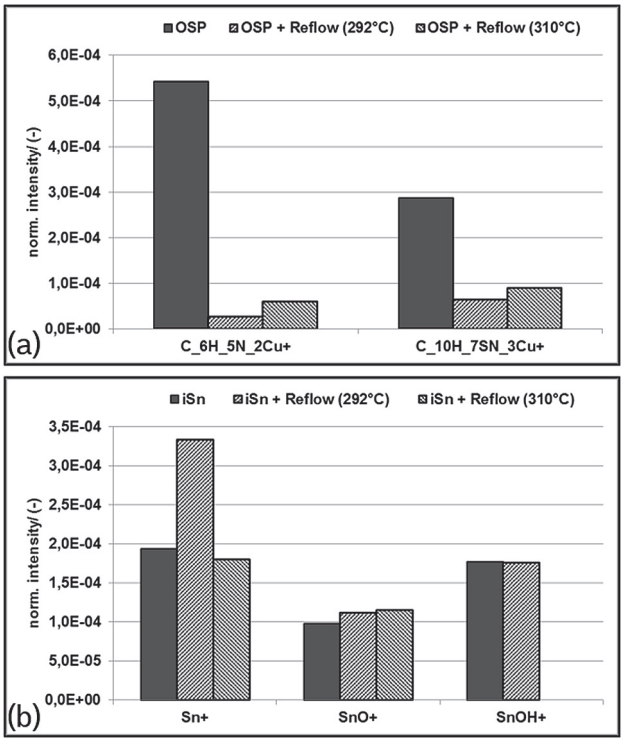

Fig. 9. ToF-SIMS normalized intensity of OSP residues (a) and iSn residues (b) within the thermal treatment by reflow with the profiles reflow (292 °C) and reflow (310 °C).

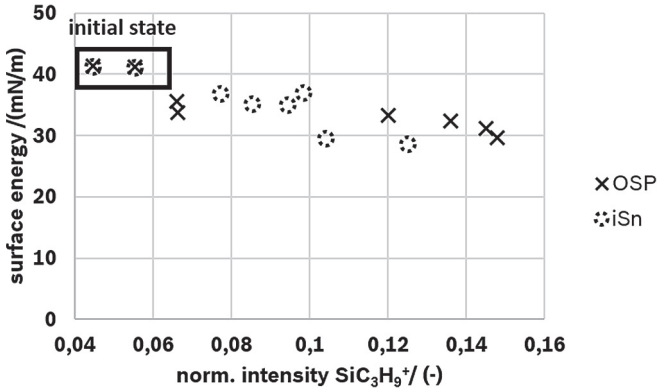

Fig. 10. Surface energy versus $SiC_3H_9^+$ normalized intensity: Based on the initial state (without OSP or iSn treatment), surface energy decreased in both configurations; while iSn configuration exhibited rapid decrease to a surface energy of 30 mN/m due to thermal treatment with reflow profile at 310 °C.

3.5. Surface model

The surface modification of the solder mask during the different process stages can be described in a surface model, summarized in Fig. 11. During all stages, no photo-oxidation of the siloxane species in form of a hydroperoxidation described by Israeli et al. [31,32] was observed. Therefore, Si 2p levels in the XPS showed that the different binding states of the organic silicon at 102.0 eV and inorganic silicon at 103.5 eV [39] exhibited increasing and nearly constant behavior, respectively. Concerning the surface energy, an increase of the polar part would have been expected if oxidation occurred. But in contrast, the surface energy measurements showed a decrease in the disperse and polar parts and seemed to converge to the surface energy level of pure PDMS [40] with increasing siloxane content at the surface. Fig. 11 concludes a surface model after each process stage in the case of OSP final finish, which does not exhibit thermal stability, derived from the XPS, ToF-SIMS and contact angle measurement results. The increase in O/C

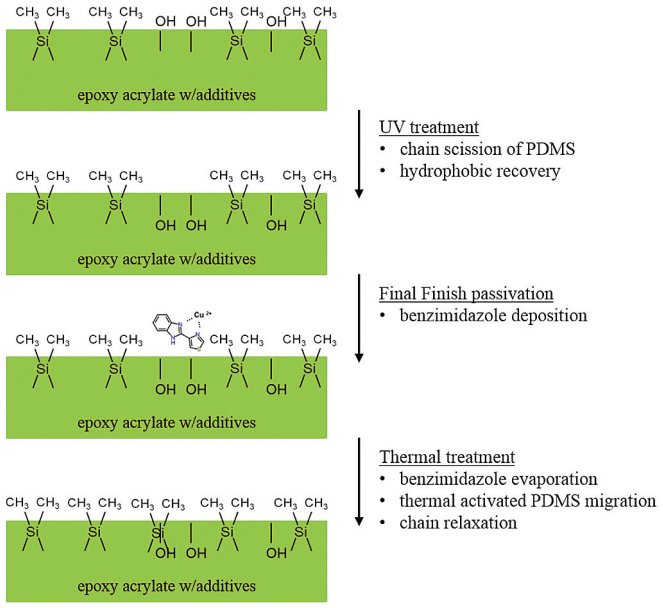

Fig. 11. Schematic surface model. Chemical surface appearance depends on the process stages. Main components of the coating system are PDMS and polar groups, as well as the final finish residues.

ratio based on XPS results, the "loss" of polar groups based on ToF-SIMS results and the decrease in surface energy correspond to a hydrophobic recovery observed by Truica-Marasecu et al. [35].

During a chemical treatment like OSP or iSn, an accumulation of final finish residues at the surface is observed. In the case of OSP, these residues lack stability within a thermal treatment, resulting in free sites for siloxane migration at elevated temperatures. Even though there are no significant changes of PDMS within iSn configurations (with and without thermal treatment) based on ToF-SIMS and XPS results compared with OSP configurations, which exhibit an increase of PDMS during the thermal treatment, the surface energy of both, the iSn and OSP configurations, tend to a surface energy of approx. 30 mN/m after the thermal treatment at 310 °C. After this stage, a resulting difference of 1 at% between the iSn and OSP configurations exists, but generates no measureable differences in the surface energy. Since the surface temperature of 260 °C within the reflow profile at 310 °C is two times higher than the glass transition temperature of the solder mask, side-group and lateral chain relaxation takes place reducing the surface energy, like observed by Andrade et al. [41]. This effect of so called ageing or hydrophobic recovery is known to exhibit no modification of the surface composition detected by XPS [42], because relaxation processes are limited to a thin surface layer. Hence, the decrease in surface energy is generated by two mechanisms: the thermally activated PDMS migration and the hydrophobic recovery via chain relaxation.

4. Conclusion

Epoxy acrylate chemistry as a typical base of photoimageable solder mask formulations has been treated under various conditions occurring in the PCB manufacturing and assembly process. Provided by XPS, increasing siloxane content at the solder mask surface is caused by any process stage due to the migration of PDMS based additives like anti-foaming and wetting agents. Detailed analysis of siloxane reactions at the surface was possible applying ToF-SIMS.

During UV treatment, no photo-oxidation like a hydroperoxidation of PDMS occurred, but UV induced chain scission and PDMS migration resulting in a decrease in surface energy, similar like hydrophobic recovery.

Final Finish passivation leads to remaining residues on the solder mask surface exhibiting different thermal stabilities within the thermal treatment reflow. In spite of measurable differences in the surface composition of iSn and OSP configurations based on XPS and ToF-SIMS results, a low energy surface of 30 mN/m in both configurations results from chain relaxation during thermal ageing, eventually.

The difference in PDMS amount between OSP and iSn configurations (after thermal ageing) of 1 at% in 10 nm depth within the solder mask surface is measured, indicating the formation of a weak boundary layer [43] and the known lack in adhesion due to PDMS residues [24] causing delamination.

Still, with respect to bonding on solder mask coated PCBs with high modulus adhesives, good adhesion was observed, independent of the iSn or OSP configuration.

References

[1] IPC-HDBK-840, IPC Association Connecting Electronics Industries, 2006.
[2] Y.-J. Park, D.-H. Lim, H.-J. Kim, D.-S. Park, I.-K. Sung, UV- and thermal-curing behaviors of dual-curable adhesives based on epoxy acrylate oligomers, Int. J. Adhes. Adhes. 29 (2009) 710–717.
[3] J.F. Rabek, Polymer Photodegradation: Mechanisms and Experimental Methods, Springer Science & Business Media, 1995.
[4] C. David, D. Baeyens-Volant, G. Delaunois, Q.L. Vinh, W. Piret, G. Geuskens,

Photo-oxidation of polymers—III: molecular weight changes in the photolysis and photo-oxidation of polystyrene, Eur. Polym. J. 14 (1978) 501–507.
[5] J. Adams, J. Goodrich, Analysis of nonvolatile oxidation products of polypropylene. II. Process degradation, J. Polym. Sci. Part A-1 Polym. Chem. 8 (1970) 1269–1277.
[6] N.S. Allen, M.C. Marin, M. Edge, D.W. Davies, J. Garrett, F. Jones, Photoinduced chemical crosslinking activity and photo-oxidative stability of amine acrylates: photochemical and spectroscopic study, Polym. Degrad. Stab. 73 (2001) 119–139.
[7] E. Yousif, R. Haddad, Photodegradation and Photostabilization of Polymers, Especially Polystyrene: Review. http://wwwspringerpluscom/content/2/1/398.
[8] M. Arra, D. Shangguan, D. Xie, J. Sundelin, T. Lepistö, E. Ristolainen, Study of immersion silver and tin printed-circuit-board surface finishes in lead-free solder applications, J. Electron Mater 33 (2004) 977–990.
[9] K.H. Tong, M.T. Ku, K.L. Hsu, Q. Tang, C.Y. Chan, K.W. Yee, The evolution of organic solderability preservative (OSP) process in PCB application, in: Microsystems, Packaging, Assembly and Circuits Technology Conference (IMPACT), 2013, pp. 43–46, 8th International 2013.
[10] T.H. Thomas, T. Kendrick, Thermal analysis of polydimethylsiloxanes. I. Thermal degradation in controlled atmospheres, J. Polym. Sci. Part A-2 Polym. Phys. 7 (1969) 537–549.
[11] D.K. Chattopadhyay, S.S. Panda, K.V.S.N. Raju, Thermal and mechanical properties of epoxy acrylate/methacrylates UV cured coatings, Prog. Org. Coat. 54 (2005) 10–19.
[12] D. Briggs, Applications of XPS in Polymer Technology, John Wiley & Sons Ltd., 1983.
[13] J.C. Vickerman, D. Briggs, ToF-SIMS: Surface Analysis by Mass Spectrometry: IM, 2001.
[14] A. Benninghoven, Chemical analysis of inorganic and organic surfaces and thin films by static time-of-flight secondary ion mass spectrometry (TOF-SIMS), Angew. Chem. Int. Ed. 33 (1994) 1023–1043.
[15] D.E. Packham, Surface energy, surface topography and adhesion, Int. J. Adhes. Adhes. 23 (2003) 437–448.
[16] J.W. McBain, D.G. Hopkins, On adhesives and adhesive action, J. Phys. Chem. 29 (1924) 188–204.
[17] G. Fourche, An overview of the basic aspects of polymer adhesion, Part I Fundam. Polym. Eng. Sci. 35 (1995) 957–967.
[18] F.M. Fowkes, Role of acid-base interfacial bonding in adhesion, J. Adhes. Sci. Technol. 1 (1987) 7–27.
[19] L. Sharpe, H. Schonhorn, Theory given direction to adhesion work: new theory is based on surface energetics, helps predict what constitutes a good adhesive, Chem. Eng. News 15 (1963) 67–68.
[20] S. Voyutskii, Adhesion and Autohesion of High Polymers, 1963.
[21] J.J. Bikerman, Causes of poor adhesion: weak boundary layers, Ind. Eng. Chem. 59 (1967) 40–44.
[22] F. Awaja, M. Gilbert, G. Kelly, B. Fox, P.J. Pigram, Adhesion of polymers, Prog. Polym. Sci. 34 (2009) 948–968.
[23] S.J. Hinder, C. Lowe, J.T. Maxted, J.F. Watts, Migration and segregation phenomena of a silicone additive in a multilayer organic coating, Prog. Org. Coat. 54 (2005) 104–112.
[24] A.T. Cheung, Delamination from process induced sources, in: Electronic Components and Technology Conference, 1999, 1999, pp. 816–822. Proceedings 49th1999.
[25] M. Ramirez, L. Henneken, S. Virtanen, Oxidation kinetics of thin copper films and wetting behaviour of copper and Organic Solderability Preservatives (OSP) with lead-free solder, Appl. Surf. Sci. 257 (2011) 6481–6488.
[26] T. Hetschel, Alterungsverhalten und Lötbarkeit der chemisch abgeschiedenen Zinn-Leiterplattenendoberfläche: Detert, 2009.
[27] Manual of contact angle measurement systems Kruess GmbH.131.
[28] M. Tsige, T. Soddemann, S.B. Rempe, G.S. Grest, J.D. Kress, M.O. Robbins, et al., Interactions and structure of poly(dimethylsiloxane) at silicon dioxide surfaces: electronic structure and molecular dynamics studies, J. Chem. Phys. 118 (2003) 5132–5142.
[29] J. Vickerman, D. Briggs, A. Henderson, The Wiley Static SIMS Library (Version 2), vol. 2, John Wiley, Chichester, 1999.
[30] C. Hofmeister, S. Maass, T. Fladung, K. Thiel, B. Mayer, Influence of copper layer on epoxy acrylate based solder mask surface chemistry and the effect on epoxy adhesion, Appl. Adhes. Sci. 3 (2015) 12.
[31] Y. Israëli, J. Lacoste, J. Cavezzan, J. Lemaire, Photo-oxidation of polydimethylsiloxane oils Part III—effect of dimethylene groups, Polym. Degrad. Stab. 42 (1993) 267–279.
[32] Y. Israeli, J.L. Philippart, J. Cavezzan, J. Lacoste, J. Lemaire, Photo-oxidation of polydimethylsiloxane oils: Part I—Effect of silicon hydride groups, Polym. Degrad. Stab. 36 (1992) 179–185.
[33] M.J. Owen, P.R. Dvornic, Silicone Surface Science, Springer, Netherlands, 2012.
[34] F. Awaja, P.J. Pigram, Surface molecular characterisation of different epoxy resin composites subjected to UV accelerated degradation using XPS and ToF-SIMS, Polym. Degrad. Stab. 94 (2009) 651–658.
[35] F. Truica-Marasescu, P. Jedrzejowski, M.R. Wertheimer, Hydrophobic recovery of vacuum ultraviolet irradiated polyolefin surfaces, Plasma Process. Polym. 1 (2004) 153–163.
[36] H.-J. Kim, K.-W. Paik, Adhesion and reliability of anisotropic conductive films (ACFs) joints on organic solderability preservatives (OSPs) metal surface finish, J. Electron Mater 37 (2008) 1003–1011.
[37] T. Hetschel, K.J. Wolter, F. Phillipp, Wettability effects of immersion tin final finishes with lead free solder, in: Electronics System-integration Technology Conference, 2008, pp. 561–566. ESTC 2008 2nd2008.
[38] B.L. Witold Paw, John Swanson, Peter Yeh, Key Characteristics of a Pb-Free OSP Process, PCB Fabrication, 2007, pp. 10–13.
[39] G. Beamson, D. Briggs, High Resolution XPS of Organic Polymers-the Science ESCA Science Database, John Wiley & Sons, Ltd, Chichester, 1992.
[40] D.K.W.R. Owens, Estimation of the surface free energy of polymers, J. Appl. Polym. Sci. 13 (1969) 1741.
[41] J.D. Andrade, DEG, L.M. Smith, Surface and Interfacial Aspects of Biomedical Polymers, Plenum Press, New York, 1985.
[42] M. Morra, EO, F. Garbassi, J. Colloid Interface Sci. 132 (1989) 475.
[43] D.E. Packham, Handbook of Adhesion, John Wiley & Sons, 2006.